ACS OMEGA

http://pubs.acs.org/journal/acsodf

Article

Colorimetric Aptasensor for the Visual and Microplate Determination of Clusterin in Human Urine Based on Aggregation Characteristics of Gold Nanoparticles

Lina Wen,[#] Xiaoyu Du,[#] Tianci Liu,[#] Wen Meng, Tao Li, Mengjie Li, and Man Zhang*

Cite This: *ACS Omega* 2023, 8, 16000−16008

Read Online

ACCESS | Metrics & More | Article Recommendations | Supporting Information

ABSTRACT: Clusterin has the potential to become the biomarker of multiple diseases, but its clinical quantitative detection methods are limited, which restricts its research progress as a biomarker. A rapid and visible colorimetric sensor for clusterin detection based on sodium chloride-induced aggregation characteristic of gold nanoparticles (AuNPs) was successfully constructed. Unlike the existing methods based on antigen−antibody recognition reactions, the aptamer of clusterin was used as the sensing recognition element. The aptamer could protect AuNPs from aggregation caused by sodium chloride, but clusterin bound with aptamer detached it from AuNPs, thereby inducing aggregation again. Simultaneously, the color change from red in the dispersed state to purple gray in the aggregated state made it possible to preliminarily judge the concentration of clusterin by observation. This biosensor showed a linear range of 0.02−2 ng/mL and good sensitivity with a detection limit of 5.37 pg/mL. The test results of clusterin in spiked human urine confirmed that the recovery rate was satisfactory. The proposed strategy is helpful for the development of label-free point-of-care testing equipment for clinical testing of clusterin, which is cost-effective and feasible.

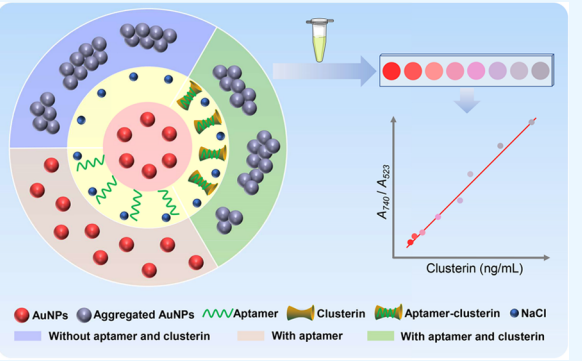

1. INTRODUCTION

Clusterin, alias of which is apolipoprotein J (ApoJ), TRPM-2, or SPG2, is an isodisaccharide protein with a molecular weight of 75−80 kDa, named for its ability to prevent protein aggregation.[1] As a secreted mammalian chaperone, clusterin has many physiological functions in vivo; for example, it can inhibit the formation of amyloid fibers, regulate DNA damage-mediated cell death, modulate cell proliferation, and adjust extracellular and intracellular proteostasis.[2−5] It also has the effects of neuroprotection, cardioprotection, anti-inflammation, food intake regulation, and so on.[6−8] Because of these important biological functions, clusterin has been found to be involved in a variety of diseases, such as ischemic brain damage-stroke, Alzheimer's disease, α-synucleinopathies, aging, neurodegeneration, osteoporosis, asthma, chronic rhinosinusitis with nasal polyps, atherosclerosis and cholesterol clearance, diabetes, obesity, pain, cancer, and cardiometabolic syndrome.[9−11] However, clusterin plays complex roles in different diseases, which has attracted more attention from researchers, although some research conclusions are controversial. Currently, clusterin is considered to be one of the biomarkers of several diseases, such as renal lupus, kidney injury, and Alzheimer's disease.[12−14] A urine proteomics study showed that clusterin might be a differential protein between diabetes patients and healthy people, which needs to be further verified by clinical research with a large sample size.[15] It can be seen that clusterin has the potential to become a biomarker of multiple diseases. For the validation of protein biomarkers, in addition to qualitative verification methods such as immunohistochemistry and Western blot, the quantification detection of the secreted protein is also particularly important. The development and establishment of quantitative detection methods for clusterin will facilitate the study of disease biomarkers.

As a ubiquitous multifunctional glycoprotein, clusterin widely exists in most tissues in the human body, which provides the possibility for detecting its concentration in body fluids to evaluate the disease process.[1] Cerebrospinal fluid, amniotic fluid, blood, and urine are commonly applied clinical test samples. In recent years, tears, saliva, and nasal secretions have also been used in clinical tests. Compared with other body fluid biological samples, urine samples have the advantages of easy access, noninvasiveness, easy preservation, and a wider range of diseases that can be indicated.[16] Therefore, urine biomarkers are effective supplements to

Received: December 18, 2022
Accepted: April 7, 2023
Published: April 24, 2023

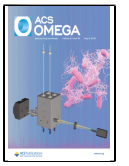

https://doi.org/10.1021/acsomega.2c08040
ACS Omega 2023, 8, 16000−16008

plasma or serum biomarkers, and exploring urine biomarkers is more conducive to promoting disease diagnosis or treatment monitoring. In that way, it is necessary to establish quantitative methods for clusterin in urine.

For the detection of clusterin, quantitative immunoprecipitation liquid chromatography/mass spectrometry (IP-LC/MS) for urine samples of cynomolgus and enzyme-linked immunosorbent assay (ELISA) analysis for nasal secretion samples of humans have been reported.[17,18] The biggest challenge these classical methods face is that the sensitivity is not high enough and the operation is not simple and fast enough. With the development of nanotechnology and sensing technology, the emergence of biosensors makes it possible to make up for the defects of traditional methods.[19−21] Label-free immunosensors that depend on electrochemistry and graphene field-effect transistor biosensors for clusterin have been developed.[22,23] The essence of these sensors is the signal amplification system based on the antigen−antibody recognition reaction, so the sensitivity of detection is significantly improved. In addition to the signal amplification system, improving the recognition response elements of target molecules is another way to build clusterin biosensors that meet the needs of clinical testing.

In addition to antibodies, aptamers are also ideal recognition elements for target molecules.[24−26] Aptamers are DNA or RNA sequences composed of specific bases. Different from the principle of the antibody-recognizing antigens, aptamers selected by systematic evolutions of ligands by exponential enrichment (SELEX) can fold into a specific secondary or tertiary structure to match the conformation of the target molecules so as to recognize the analytes and realize biosensing.[27] Compared with antibodies, aptamers have certain advantages: high thermal/chemical stability, a wide range of recognizable targets, low immunogenicity, low detection cost, and others.[28,29] For clinical applications, simple and rapid detection methods are preferred on the premise of ensuring sensitivity. As one of the most significant characteristics, the localized surface plasmon resonance (LSPR) of AuNPs can induce a shift in the visible absorption spectrum to change the color of the aqueous solution, which makes colorimetric detection practicable.[30] Some sensors based on modified AuNP probes for the direct testing of Pb^{2+} and other targets in the environment have been reported.[31] Colorimetry principle based on AuNPs is also widely used in clinical testing because it can judge the concentration of analytes through color discrimination, for example, with an early pregnancy (human chorionic gonadotropin, HCG) detection kit. In recent years, colloidal gold-based colorimetric aptamer sensors have been widely concerned in the field of biological analysis,[32,33] which provides a new direction for the establishment of a fast and convenient clinical testing method for clusterin.[34]

In this work, depending on the aggregation characteristics of gold nanoparticles (AuNPs) induced by sodium chloride, a label-free, visual, and rapid colorimetric aptasensor in a microplate for detecting the concentration of clusterin in human urine was established. Ultraviolet−visible (UV−vis) absorption spectra were efficient tools and adopted to clarify the colorimetric properties of the sensing process and further prove the sensing principle.[35,36] The concentration of clusterin is linearly correlated with the aggregation degree of AuNPs and the corresponding absorbance decrease and color change, which can be used to quantitatively analyze clusterin. This novel sensing strategy of clusterin based on aptamer recognition elements and AuNP probes may provide a reference for exploring the point-of-care testing (POCT) device and validating clusterin as a biomarker of diseases.

2. MATERIALS AND METHODS

2.1. Materials and Reagents. Tetrachloroauric acid ($HAuCl_4{\cdot}4H_2O$) was purchased from Aladdin Industrial Corporation (Shanghai, China). Trisodium citrate and sodium chloride were purchased from Sinopharm Chemical Reagent Co., Ltd. (Shanghai, China). The reagents were of analytical reagent grade. Two sequences clusterin 1: 5′-CTCCTCTGACTGTAACCACGTTAGGCGAGAACATGT-CAGTACGTCGACGTTCTACTTGCTGCATAGGTAGTC-CAGAAGCC-3′,[37] and clusterin 2: 5′-CTCCTCTGACTG-TAACCACGTTAGGCGAGAACATGTCAGT-3′ were employed for optimizing the aptamer of clusterin and synthesized by Sangon Biotech Co., Ltd (Shanghai, China). All working solutions were prepared with doubly distilled water.

2.2. Instrumentation. The UV−vis absorption spectra of AuNPs were measured by an Agilent Cary 3500 spectrophotometer (Agilent Technologies) with a 10 mm wide fused silica cuvette at room temperature. The morphology of AuNPs was observed on a JEM-1400 transmission electron microscope (TEM) (JEOL, Japan). Microplate detection was carried out with a SPARK10M microplate reader (TECAN).

2.3. Synthesis and Characterization of AuNPs. AuNPs were synthesized by the classical method of $HAuCl_4$ reduction according to the reported protocol.[38] In brief, the $HAuCl_4$ aqueous solution (50 mL, 1 mM) was put into the flask, heated, and stirred. After boiling, the sodium citrate aqueous solution (5 mL, 38.8 mM) was quickly injected. When the color developed into claret, the aqueous solution was gradually cooled to room temperature. The maximum absorbance was at 523 nm, as reflected by the UV−vis absorption spectrum (see Figure S1A), and the average particle size of AuNPs was about 18 nm, as revealed by TEM (see Figure S1B). The concentration was calculated to be 5 nmol/L according to the Lambert−Beer law.[39]

2.4. Optimization of Biosensing Conditions. First, the effects of different concentrations of sodium chloride on the maximum absorption of AuNPs were explored to determine the optimum sodium chloride concentration. Second, two nucleotide sequences composed of different bases were used to screen the optimal aptamer of clusterin, of which clusterin 1 was derived from the previous report.[40] The concentration of AuNPs and sodium chloride was fixed in the system, and different concentrations of clusterin were added under the same concentration of different aptamer sequences. The maximum absorbance with the changing of the clusterin concentrations was compared among different aptamer systems, and the aptamer with the most sensitive change of absorbance was confirmed to be the optimal one. Third, the influence of different aptamer concentrations on the maximum absorption of the AuNPs−sodium chloride system, and the incubation time for the aptamer and sodium chloride with AuNPs was investigated respectively to confirm the optimized detection conditions.

2.5. Protocol for Colorimetric Sensing of Clusterin. At room temperature, 1 μL of a 100 μmol/L clusterin aptamer solution was mixed with 200 μL of AuNPs solution and incubated for 5 min. Then, 2 μL of a 4 mol/L NaCl solution was added and mixed. After that, a series of different densities

https://doi.org/10.1021/acsomega.2c08040
ACS Omega 2023, 8, 16000−16008

Scheme 1. Principle of Colorimetric Sensing for Clusterin in Urine Based on Aptamer and AuNPs

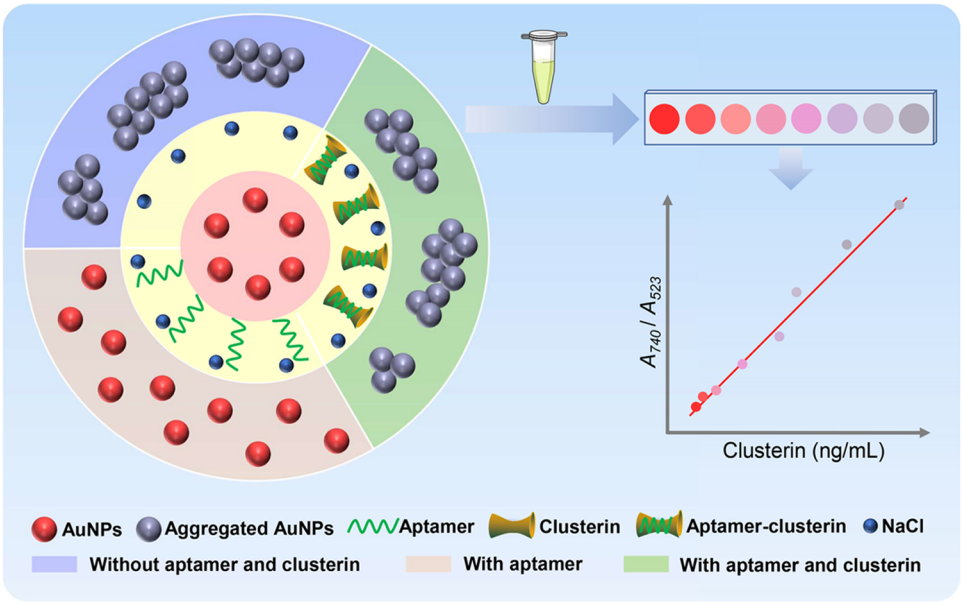

of clusterin were added to make the final concentrations range from 0.005 to 2 ng/mL. The solutions were transferred into the microplate well, homogenized, and equilibrated for 5 min. The UV−vis absorption spectra were recorded over the 400−800 nm wavelength range by a microplate reader.

2.6. Colorimetric Detection for Clusterin in Urine Samples. Urine samples were collected from volunteers with diabetes. Informed consent has been signed before collecting urine samples. The urine samples were centrifuged at 3000 rpm for 10 min, and the supernatant was taken for use. After 200 times dilution with doubly distilled water, 1 μL of sample was added into the AuNPs−aptamer−NaCl mixture system for the UV−vis absorption spectra measurement according to the above protocol.

3. RESULTS AND DISCUSSION

3.1. Principle of the Colorimetric Sensing. The mechanism of the colorimetric aptasensor for detecting clusterin in human urine based on AuNPs is shown in Scheme 1. For pure AuNPs in a dispersed state, the aqueous solution is red. In the absence of aptamer and clusterin, sodium chloride can induce the aggregation of AuNPs, and the solution system turned purple gray. In the presence of aptamer, the nitrogen bases of aptamer can adsorb onto the surface of AuNPs through noncovalent interaction. As a huge negative electricity group, aptamer disperses AuNPs by electrostatic repulsion. Sodium chloride has little effect on AuNPs protected by aptamer and the color of the aqueous solution remains red. However, when clusterin appears, aptamer DNA specifically binds to the spatial sites of clusterin and separates away from the AuNPs surface. Without the protection of the negatively charged group, AuNPs are exposed to sodium chloride and aggregate again with the solution color changing from red to purple gray. The degree of aggregation is directly related to the concentration of clusterin and is visible to the naked eye.

3.2. Characterization of the Aptasensor. The UV−vis absorption spectra were adopted to clarify the colorimetric properties of the sensing process and further prove the sensing principle. The absorption spectra of AuNPs under different conditions are shown as Figure 1A. As expected, compared with AuNPs in the dispersed state, the maximum absorption

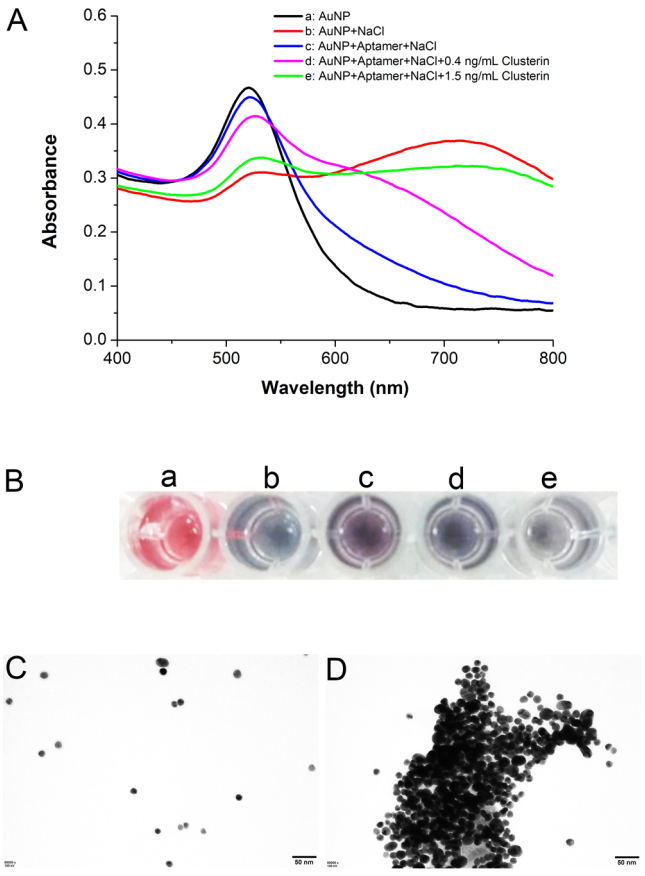

Figure 1. (A) UV−vis absorption spectra of AuNPs under different experimental conditions. There were 5 nmol/L AuNPs, 32 mmol/L NaCl, and 0.6 μmol/L aptamer in the solution system. (B) Colorimetric diagram corresponding to absorption spectra in (A). (C) TEM images of 5 nmol/L AuNPs−0.6 μmol/L aptamer−32 mmol/L NaCl. (D) TEM images of 5 nmol/L AuNPs−0.6 μmol/L aptamer−32 mmol/L NaCl−2 ng/mL clusterin.

https://doi.org/10.1021/acsomega.2c08040
ACS Omega 2023, 8, 16000−16008

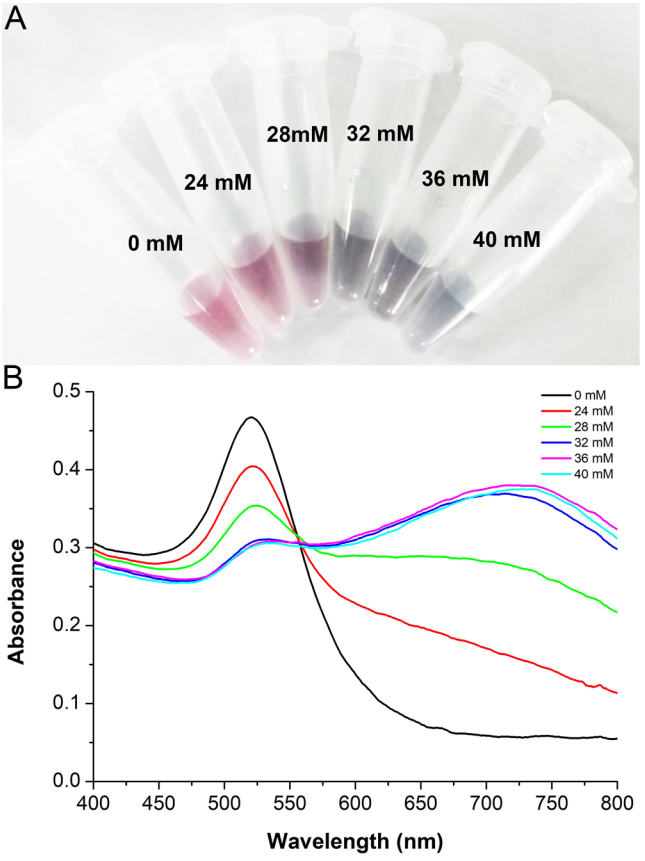

Figure 2. Effects of different concentrations of NaCl on the color (A) and absorption spectra (B) of AuNPs. There were 5 nmol/L AuNPs in the reaction system.

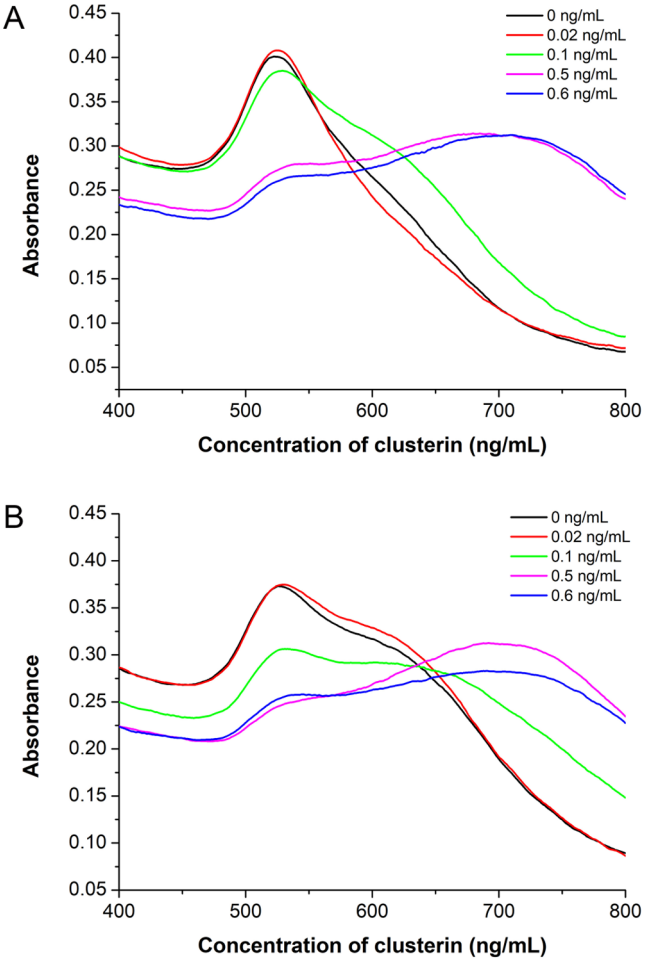

Figure 3. Effects of different concentrations of clusterin on the absorption spectra of AuNPs−clusterin 1 sequence−NaCl solution system (A) and AuNPs−clusterin 2 sequence−NaCl solution system (B). There were 5 nmol/L AuNPs, 0.4 μmol/L aptamer, and 32 mmol/L NaCl in the reaction system.

intensity around 523 nm decreased significantly and the absorption peak appeared at about 740 nm in the aggregation state induced by sodium chloride. Subsequently, the absorption peak near 523 nm was obviously enhanced and the absorption intensity around 740 nm evidently decreased in the AuNP−aptamer−NaCl system compared with that in the AuNP−NaCl system. On this basis, the maximum absorbance in the AuNP−aptamer−NaCl−clusterin system gradually decreased with the increase of the clusterin concentration.

Accordingly, the change of color is exhibited as Figure 1B. In this experimental system, the dispersed AuNPs are red and the aggregated AuNPs induced by sodium chloride are gray. For the system with the state of partial dispersion and partial aggregation, the degree of aggregation gradually increased with the increasing protein concentration, and the color presented purplish red, light purplish red, and light purplish gray in turn.

The morphological changes reflected by TEM proved the basic principle again. As shown in Figure 1C, AuNPs in the AuNP−aptamer−NaCl system and AuNP−aptamer−NaCl−clusterin system were dispersed and aggregated, respectively.

3.3. Optimization of Experimental Conditions.

3.3.1. Determination of the Optimum Salt Concentration. It can be seen from Figure 2A that when the sodium chloride concentration of the system was lower than 24 mmol/L, the solution remained red. At 28 mmol/L, the color changed from red to purple. At 32 mmol/L, the color turned gray and deepening was not obvious with the increasing concentration of salts. At the same time, the absorption peak around 523 nm gradually decreased with a red-shift in the system, as shown in Figure 2B. The change of absorption peak had little difference from 32 mmol/L, indicating that AuNPs in the system had been completely aggregated. Because too high salt concentration may interfere with the sensitivity of the detection system, the optimal salt concentration was considered to be 32 mmol/L.

3.3.2. Optimization of the Clusterin Aptamer. The sequence clusterin 1, which has been reported to identify clusterin in A549 cells, was employed to construct and optimize the biosensing system. It can be seen that with the presence of sodium chloride and clusterin 1 sequence, the maximum absorbance of AuNPs near 523 nm decreased with the increasing concentration of clusterin, indicating that the clusterin 1 sequence bound with clusterin and could be used as a clusterin aptamer (see Figure 3A). However, there were 80 bases in this sequence, which was not conducive to improving the detection sensitivity of a colorimetric biosensor based on AuNPs. Furthermore, the clusterin 1 sequence was suspected to bind with other proteins in A549 cells, and the specificity remained to be improved. Therefore, the sequence clusterin 2 composed of 40 bases was tested. With the presence of sodium chloride and clusterin 2 sequence, the maximum absorbance of AuNPs near 523 nm also decreased with the increasing concentration of clusterin, but the maximum absorbance

https://doi.org/10.1021/acsomega.2c08040
ACS Omega 2023, 8, 16000−16008

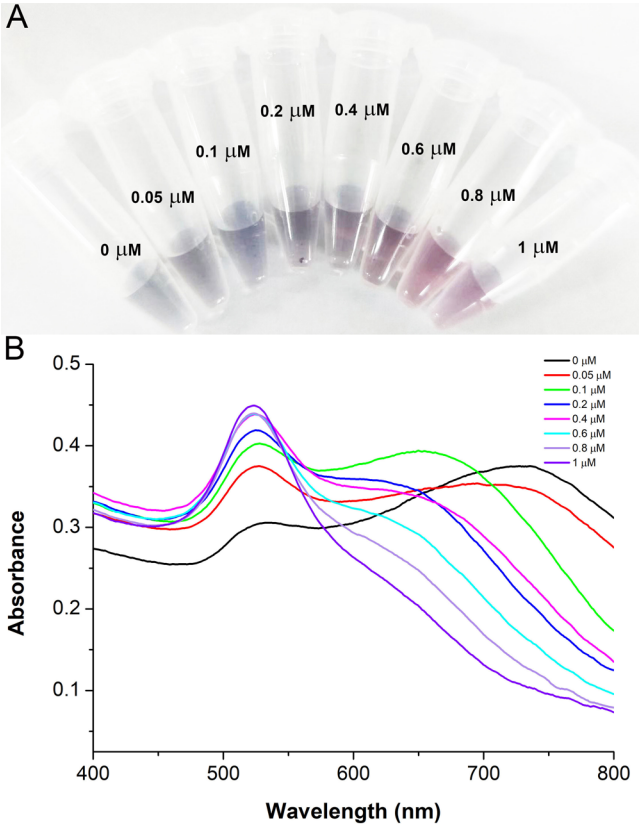

Figure 4. Effects of different concentrations of aptamer on the color (A) and absorption spectra (B) of the AuNPs−NaCl solution system. There were 5 nmol/L AuNPs and 32 mmol/L NaCl in the reaction system.

changed more obviously with 0.1 ng/mL clusterin compared with that of clusterin 2 sequence, indicating that the clusterin 2 sequence might have better sensitivity (see Figure 3B). In conclusion, the clusterin 2 sequence was selected to be the aptamer of clusterin.

3.3.3. Determination of the Optimum Aptamer Concentration. The color variation and absorption spectra of the AuNPs solution incubated with clusterin aptamer at different concentrations in the system with 40 mmol/L final concentration of sodium chloride are shown in Figure 4A,B. Without the aptamer, the sodium chloride−AuNPs solution was gray, and there was a strong absorption peak at ∼740 nm and a weak absorption peak around 523 nm reflected by the UV−vis spectra, conforming to the aggregation characteristics of AuNPs. With the increase of the aptamer concentration, the more molecules adsorbed on the surface of AuNPs, and the stronger the protective effects. Therefore, AuNPs gradually disintegrated and the color converted from gray to red. Meanwhile, the peak near 523 nm gradually increased, and the peak at ∼740 nm gradually disappeared with a blue-shift. When the concentration was 0.4 μmol/L, the protective effect was initially shown as purplish red. With the aptamer concentration increasing to 0.8 μmol/L, the color turned light red and did not obviously change when the concentration continued to increase, indicating that AuNPs had been protected sufficiently by the aptamer. From 0.4 to 0.8 μmol/L, the maximum absorption intensity had little difference. Considering the sensitivity of detection, 0.6 μmol/L was used as the optimal incubation concentration of the aptamer.

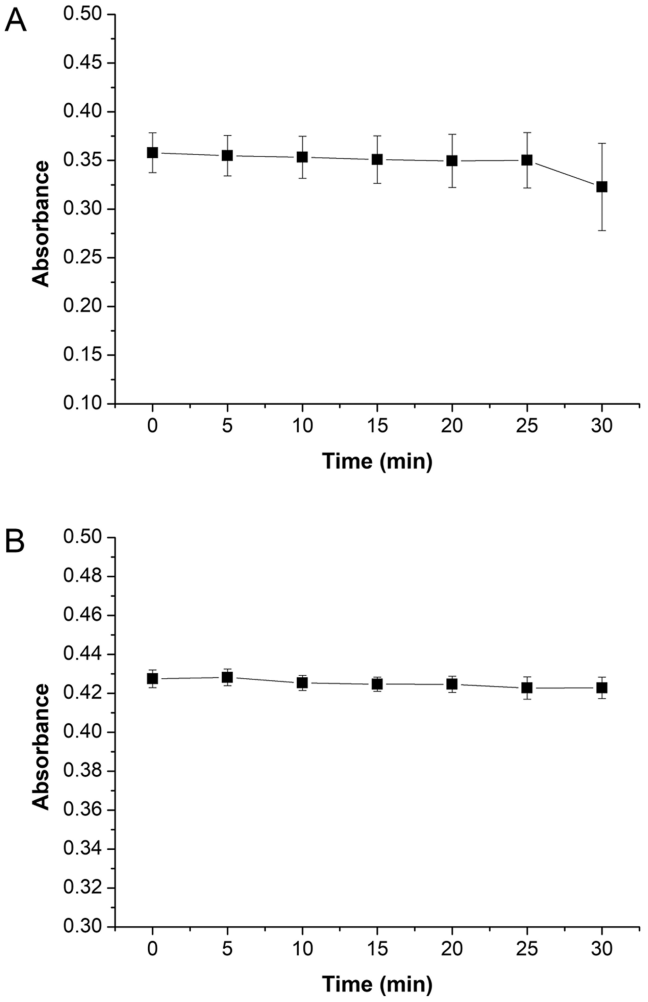

Figure 5. Effects of different reaction times between AuNPs and NaCl (A) and AuNPs and aptamer (B) on the maximum absorbance of AuNPs in the solution system. The concentrations of AuNPs, aptamer, and NaCl were 5 nmol/L, 0.6 μmol/L, and 32 mmol/L, respectively.

3.3.4. Determination of the Optimum Reaction Time. The incubation times for sodium chloride with AuNPs and the aptamer with AuNPs were optimized. It can be concluded from Figure 5A that as time went on, within 25 min, the aggregation degree of AuNPs induced by sodium chloride did not change significantly. The maximum absorbance decreased slightly from 0 to 20 min and remained unchanged from 20 to 25 min, but decreased obviously from 25 to 30 min. Therefore, to minimize the impact of reaction time on the sensing system, the incubation time of sodium chloride was selected as 5 min. Different from sodium chloride, incubation time rarely affected the interaction between aptamer and AuNPs, as shown in Figure 5B. Thus, it was suggested that the reaction time of the aptamer with AuNPs was controlled at 5 min and that the determination of clusterin should be carried out as soon as possible after sodium chloride is added to the system.

3.4. Sensitivity of the Colorimetric Aptasensor for Clusterin Detection. According to the protocol for colorimetric sensing, the UV−vis absorbance spectra of the sensing system with different concentrations of clusterin were measured. As shown in Figure 6A, the increase in the concentration of clusterin induced a gradual decline in the

https://doi.org/10.1021/acsomega.2c08040
ACS Omega 2023, 8, 16000−16008

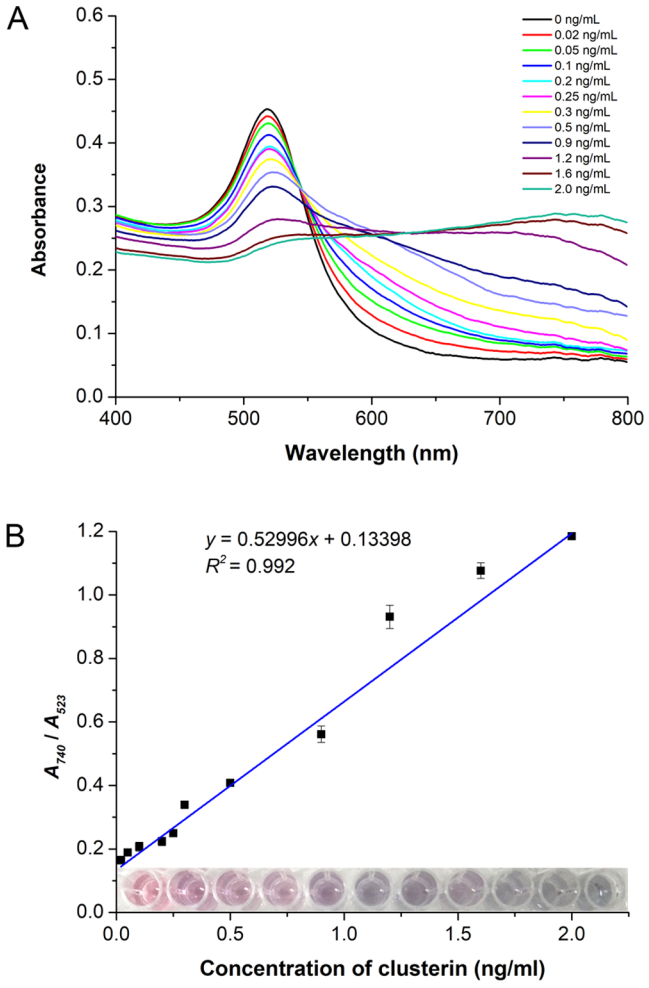

Figure 6. Sensitivity of the proposed aptasensor for clusterin determination. (A) UV−vis absorption spectra of AuNPs in the presence of different concentrations of clusterin. (B) Linear range of the standard curve and the corresponding color changes. There were 5 nmol/L AuNPs, 0.6 μmol/L aptamer, and 32 mmol/L NaCl in the reaction system.

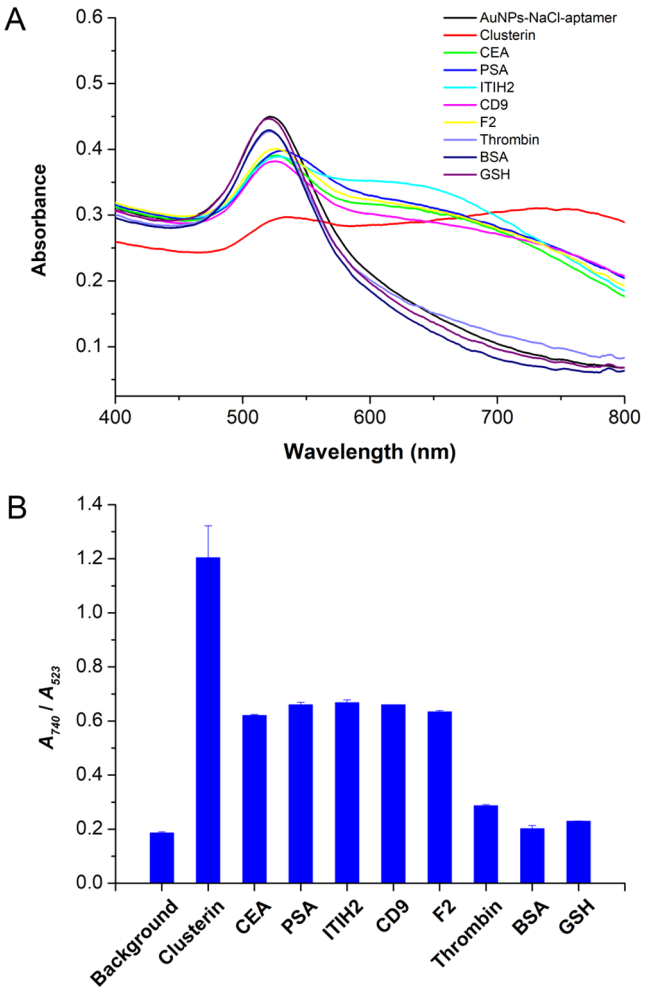

Figure 7. Specificity of the proposed aptasensor for clusterin determination. (A) UV−vis absorption spectra of AuNPs in the presence of interfering protein CEA, PSA, ITIH2, CD9, F2, thrombin, BSA, and GSH in a concentration of 1 ng/mL. (B) Absorbance ratio of 740−523 nm of the system induced by eight interfering substances and clusterin. There were 5 nmol/L AuNPs, 0.6 μmol/L aptamer, and 32 mmol/L NaCl in the reaction system.

absorption intensity at ∼523 nm, with the colors transforming from red to gray gradually. When the concentration was increased to 2 ng/mL, the absorption peak near 523 nm almost disappeared, while a new absorption peak appeared at about 740 nm. The ratio of the absorption intensity of 740 and 523 nm was positively correlated with the concentration of clusterin over the range of 0.02−2 ng/mL, with the color of AuNPs gradually converting from red to light gray (see Figure 6B). In this way, the linear regression equation was y = 0.52996x + 0.13398 (R^2 = 0.992), and the limit of detection (LOD) of 5.37 pg/mL was calculated according to the 3σ rule described by the International Union of Pure and Applied Chemistry (IUPAC).[40]

Different determination methods for the quantitation of clusterin are generalized briefly in Table 1. Compared with previously reported biosensor detection methods based on recognition elements of antibodies and the classical quantitative method of ELISA, this sensor method has a better sensitivity than ELISA and the advantages of simplicity, fastness, and low cost.

3.5. Selectivity of Colorimetric Aptasensor for Clusterin Analysis. Selectivity is an important index to evaluate the practical application value of biosensors.[41] There may be a variety of proteins in the complex biological system of urine. To verify the selectivity of the aptasensor for clusterin (1 ng/mL) detection, eight disruptors including carcinoem-

Table 1. Comparison between the Proposed Colorimetric Aptasensor and Other Techniques for Clusterin Detection

methods	recognition elements	LOD	linear range	time	references
immunosensor based on electrochemistry	antibody	1 pg/mL	1−100 pg/mL	>24 h	22
graphene field-effect transistor biosensors	antibody	300 fg/mL	1−100 pg/mL	>5 h	23
ELISA	antibody	22.5 pg/mL	0.2344−15 ng/mL	1.5 h	18
colorimetric aptasensor based on AuNPs	aptamer	5.37 pg/mL	0.02−2 ng/mL	15 min	this work

https://doi.org/10.1021/acsomega.2c08040
ACS Omega 2023, 8, 16000−16008

Table 2. Analytical Results for Clusterin in Urine Samples of Diabetic Using the Proposed Method and ELISA

sample	colorimetric (ng/mL)	ELISA (ng/mL)	spiked (ng/mL)	found (ng/mL)	recovery (%)	RSD (%)
1	87.35 ± 1.72	88.69 ± 0.06	40	39.74 ± 2.22	99.36 ± 2.22	1.86
2	45.85 ± 2.02	46.96 ± 0.06	30	28.01 ± 4.02	93.38 ± 4.02	4.51
3	59.51 ± 6.13	60.01 ± 0.10	30	28.96 ± 4.72	96.53 ± 4.72	4.1

bryonic antigen (CEA), prostate-specific antigen (PSA), inter α-globulin inhibitor H2 (ITIH2), CD9, coagulation factor II (F2), thrombin, bovine albumin (BSA), and glutathione (GSH) (each at 1 ng/mL) were randomly supposed to be the potential interfering proteins and detected following the same experimental process. As exhibited in Figure 7A, clusterin caused a remarkable variation in the absorption spectra for AuNPs. Comparatively speaking, the absorption spectra changes for AuNPs induced by the other eight interference substances were not as obvious as that of clusterin. The absorbance ratio of 740−523 nm of the system caused by clusterin, CEA, PSA, ITIH2, CD9, F2, thrombin, BSA, and GSH is shown as Figure 7B. It can be concluded that other substances had negligible interferences on the clusterin sensing system, and this assay might be applied for clusterin detection with good selectivity.

3.6. Application in Clinical Urine Samples. To assess the practical applicability of the proposed colorimetric aptasensor, it was used to detect the concentration of clusterin in clinical urine samples. Previous results on the basis of mass spectrometry showed that the abundance of clusterin in the urine of patients with diabetes was lower than that of healthy people, so the concentration of clusterin in the urine of diabetes volunteers was detected by the aptasensor and ELISA methods, respectively. As shown in Table 2, both the analytical results obtained from colorimetric sensing and the values determined by ELISA were expressed as mean ± RSD (%). For the recovery experiments, the spiked recoveries fluted between 93.38 and 99.36%, with the relative standard deviation (RSD) range of 1.86−4.51%. Thus, it can be seen that the developed colorimetric aptasensor was practicable for the rapid analysis of clusterin in real urine samples.

4. CONCLUSIONS

To sum up, a quick, convenient, and cost-effective label-free colorimetric analysis strategy for the quantitative detection of clusterin in urine was successfully developed based on the probes of unmodified AuNPs and recognition elements of clusterin aptamer. The colorimetric sensing mechanism is that aptamers can protect AuNPs from the aggregation induced by sodium chloride, and clusterin can indirectly affect the aggregation of AuNPs by binding to aptamers. The aptasensor had good selectivity with a linear range of 0.02−2 ng/mL and a LOD of 5.37 pg/mL. Moreover, the assay was successfully applied to clinical urine sample determination of diabetes patients and the recovery met the requirements of the methodological investigation. This method is visible, specific, highly efficient, and easy to perform, which may promote the discovery, validation, and clinical application of biomarkers.

■ ASSOCIATED CONTENT

Supporting Information

The Supporting Information is available free of charge at https://pubs.acs.org/doi/10.1021/acsomega.2c08040.

UV−vis absorption spectrum of AuNPs and TEM images of AuNPs (PDF)

■ AUTHOR INFORMATION

Corresponding Author

Man Zhang − *Beijing Key Laboratory of Urinary Cellular Molecular Diagnostics, Beijing 100038, China; Clinical Laboratory Medicine, Beijing Shijitan Hospital, Capital Medical University, Beijing 100038, China; Clinical Laboratory Medicine, Peking University Ninth School of Clinical Medicine, Beijing 100038, China;* orcid.org/0000-0001-5166-6804; Email: zhangman@bjsjth.cn

Authors

Lina Wen − *Beijing Key Laboratory of Urinary Cellular Molecular Diagnostics, Beijing 100038, China; Department of Clinical Nutrition, Beijing Shijitan Hospital, Capital Medical University, Beijing 100038, China*

Xiaoyu Du − *Beijing Key Laboratory of Urinary Cellular Molecular Diagnostics, Beijing 100038, China; Clinical Laboratory Medicine, Peking University Ninth School of Clinical Medicine, Beijing 100038, China*

Tianci Liu − *Beijing Key Laboratory of Urinary Cellular Molecular Diagnostics, Beijing 100038, China; Clinical Laboratory Medicine, Beijing Shijitan Hospital, Capital Medical University, Beijing 100038, China*

Wen Meng − *Department of Infection Prevention and Control, Peking University People's Hospital, Beijing 100044, China*

Tao Li − *Beijing Key Laboratory of Urinary Cellular Molecular Diagnostics, Beijing 100038, China; Clinical Laboratory Medicine, Beijing Shijitan Hospital, Capital Medical University, Beijing 100038, China*

Mengjie Li − *Beijing Key Laboratory of Urinary Cellular Molecular Diagnostics, Beijing 100038, China; Clinical Laboratory Medicine, Peking University Ninth School of Clinical Medicine, Beijing 100038, China*

Complete contact information is available at: https://pubs.acs.org/10.1021/acsomega.2c08040

Author Contributions

#L.W., X.D., and T. Liu contributed equally to the work. M.Z. was responsible for conceptualization, data curation, formal analysis, funding acquisition, methodology, project administration, and resources. L.W., X.D., and T. Liu performed the investigation, methodology, software, supervision, validation, visualization, and writing the original draft, reviewing, and editing. W.M., T. Li, and M.L. were responsible for the investigation and validation.

Funding

This project was financially supported by the Open Research Funding of the Beijing Key Laboratory of Urinary Cellular Molecular Diagnostics (2020-KF18).

Notes

The authors declare no competing financial interest.

■ ABBREVIATIONS

ApoJ, apolipoprotein J; SELEX, systematic evolution of ligands by exponential enrichment; LSPR, localized surface plasmon

https://doi.org/10.1021/acsomega.2c08040
ACS Omega 2023, 8, 16000−16008

resonance; HCG, human chorionic gonadotropin; IUPAC, International Union of Pure and Applied Chemistry; CEA, carcinoembryonic antigen; PSA, prostate-specific antigen; ITIH2, inter α-globulin inhibitor H2; F2, coagulation factor II

REFERENCES

(1) Rodríguez-Rivera, C.; Garcia, M. M.; Molina-Álvarez, M.; González-Martín, C.; Goicoechea, C. Clusterin: Always protecting. synthesis, function and potential issues. *Biomed. Pharmacother.* **2021**, *134*, No. 111174.

(2) Liu, X.; Che, R. B.; Liang, W. P.; Zhang, Y.; Wu, L. Y.; Han, C.; Lu, H.; Song, W. H.; Wu, Y. L.; Wang, Z. Clusterin transduces Alzheimer-risk signals to amyloidogenesis. *Signal Transduction Targeted Ther.* **2022**, *7*, 325.

(3) Ming, X.; Bao, C. Y.; Hong, T.; Yang, Y.; Chen, X. B.; Jung, Y. S.; Qian, Y. J. Clusterin, a novel DEC1 target, modulates DNA damage-mediated cell death. *Mol. Cancer Res.* **2018**, *16*, 1641−1651.

(4) Praharaj, P. P.; Patra, S.; Panigrahi, D. P.; Patra, S. K.; Bhutia, S. K. Clusterin as modulator of carcinogenesis: A potential avenue for targeted cancer therapy. *Biochim. Biophys. Acta* **2021**, *1875*, No. 188500.

(5) Satapathy, S.; Wilson, M. R. The dual roles of clusterin in extracellular and intracellular proteostasis. *Trends Biochem. Sci.* **2021**, *46*, 652−660.

(6) De Miguel, Z.; Khoury, N.; Betley, M. J.; Lehallier, B.; Willoughby, D.; Olsson, N.; Yang, A. C.; Hahn, O.; Lu, N.; Vest, R. T.; Bonanno, L. N.; Yerra, L.; Zhang, L.; Saw, N. L.; Fairchild, J. K.; Lee, D.; Zhang, H.; McAlpine, P. L.; Contrepois, K.; Shamloo, M.; Elias, J. E.; Rando, T. A.; Wyss-Coray, T. Exercise plasma boosts memory and dampens brain inflammation via clusterin. *Nature* **2021**, *600*, 494−499.

(7) Bass-Stringer, S.; Ooi, J. Y. Y.; McMullen, J. R. Clusterin is regulated by IGF1-PI3K signaling in the heart: implications for biomarker and drug target discovery, and cardiotoxicity. *Arch. Toxicol.* **2020**, *94*, 1763−1768.

(8) Pucci, S.; Greggi, C.; Polidoro, C.; Piro, M. C.; Celi, M.; Feola, M.; Gasbarra, E.; Iundusi, R.; Mastrangeli, F.; Novelli, G.; Orlandi, A.; Tarantino, U. Clusterin silencing restores myoblasts viability and down modulates the inflammatory process in osteoporotic disease. *J. Transl. Med.* **2019**, *17*, 118.

(9) Spatharas, P. M.; Nasi, G. I.; Tsiolaki, P. L.; Theodoropoulou, M. K.; Papandreou, N. C.; Hoenger, A.; Trougakos, I. P.; Iconomidou, V. A. Clusterin in Alzheimer's disease: An amyloidogenic inhibitor of amyloid formation? *Biochim. Biophys. Acta* **2022**, *1868*, No. 166384.

(10) Kalvaityte, U.; Matta, C.; Bernotiene, E.; Pushparaj, P. N.; Kiapour, A. M.; Mobasheri, A. Exploring the translational potential of clusterin as a biomarker of early osteoarthritis. *J. Orthop. Transl.* **2022**, *32*, 77−84.

(11) Wilson, M. R.; Zoubeidi, A. Clusterin as a therapeutic target. *Expert Opin. Ther. Targets* **2017**, *21*, 201−213.

(12) Wu, C. Y.; Yang, H. Y.; Chien, H. P.; Tseng, M. H.; Huang, J. L. Urinary clusterin-a novel urinary biomarker associated with pediatric lupus renal histopathologic features and renal survival. *Pediatr. Nephrol.* **2018**, *33*, 1189−1198.

(13) Sandelius, Å.; Basak, J.; Hölttä, M.; Sultana, S.; Hyberg, G.; Wilson, A.; Andersson, P.; Söderberg, M. Urinary kidney biomarker panel detects preclinical antisense oligonucleotide-induced tubular toxicity. *Toxicol. Pathol.* **2020**, *48*, 981−993.

(14) Shi, X.; Xie, B.; Xing, Y.; Tang, Y. Plasma clusterin as a potential biomarker for Alzheimer's disease-a systematic review and meta-analysis. *Curr. Alzheimers Res.* **2019**, *16*, 1018−1027.

(15) Chu, L.; Fu, G.; Meng, Q.; Zhou, H.; Zhang, M. Identification of urinary biomarkers for type 2 diabetes using bead-based proteomic approach. *Diabetes Res. Clin. Pract.* **2013**, *101*, 187−193.

(16) Trindade, F.; Barros, A. S.; Silva, J.; Vlahou, A.; Falcão-Pires, I.; Guedes, S.; Vitorino, C.; Ferreira, R.; Leite-Moreira, A.; Amado, F.; Vitorino, R. Mining the biomarker potential of the urine peptidome: from amino acids properties to proteases. *Int. J. Mol. Sci.* **2021**, *22*, 5940.

(17) Gautier, J. C.; Zhou, X. B.; Yang, Y.; Gury, T.; Qu, Z.; Palazzi, X.; Léonard, J. F.; Slaoui, M.; Veeranagouda, Y.; Guizon, I.; Boitier, E.; Filali-Ansary, A.; van den Berg, B.H.J.; Poetz, O.; Joos, T.; Zhang, T. Y.; Wang, J. F.; Detilleux, P.; Li, B. Evaluation of novel biomarkers of nephrotoxicity in Cynomolgus monkeys treated with gentamicin. *Toxicol. Appl. Pharmacol.* **2016**, *303*, 1−10.

(18) Huang, Y.; Wang, M.; Hong, Y.; Bu, X.; Luan, G.; Wang, Y.; Li, Y.; Lou, H.; Wang, C.; Zhang, L. Reduced expression of antimicrobial protein secretory leukoprotease inhibitor and clusterin in chronic rhinosinusitis with nasal polyps. *J. Immunol. Res.* **2021**, *2021*, No. 1057186.

(19) Li, Y. X.; Zeng, R. J.; Wang, W. J.; Xu, J. H.; Gong, H. X.; Li, L.; Li, M. J.; Tang, D. P. Size-controlled engineering photoelectrochemical biosensor for human papillomavirus-16 based on CRISPR-Cas12a-induced disassembly of Z-scheme heterojunctions. *ACS Sens.* **2022**, *7*, 1593−1601.

(20) Yu, Z. C.; Gong, H. X.; Xu, J. H.; Li, Y. X.; Zeng, Y. Y.; Liu, X. L.; Tang, D. P. Exploiting photoelectric activities and piezoelectric properties of $NaNbO_3$ semiconductors for point-of-care immunoassay. *Anal. Chem.* **2022**, *94*, 3418−3426.

(21) Gao, Y.; Zeng, Y. Y.; Liu, X. L.; Tang, D. P. Liposome-mediated in situ formation of Type-I heterojunction for amplified photoelectrochemical immunoassay. *Anal. Chem.* **2022**, *94*, 4859−4865.

(22) Islam, K.; Damiati, S.; Sethi, J.; Suhail, A.; Pan, G. Development of a label-free immunosensor for clusterin detection as an Alzheimer's biomarker. *Sensors* **2018**, *18*, 308.

(23) Bungon, T.; Haslam, C.; Damiati, S.; O'Driscoll, B.; Whitley, T.; Davey, P.; Siligardi, G.; Charmet, J.; Awan, S. A. Graphene FET sensors for Alzheimer's disease protein biomarker clusterin detection. *Front. Mol. Biosci.* **2021**, *8*, No. 651232.

(24) Lv, S. Z.; Zhang, K. Y.; Zhu, L.; Tang, D. P. ZIF-8-assisted NaYF4: Yb, Tm@ZnO converter with exonuclease III-Powered DNA walker for near-infrared light responsive biosensor. *Anal. Chem.* **2020**, *92*, 1470−1476.

(25) Lv, S. Z.; Zhang, K. Y.; Zeng, Y. Y.; Tang, D. P. Double photosystems-based 'Z-scheme' photoelectrochemical sensing mode for ultrasensitive detection of disease biomarker accompanying 3D DNA walker. *Anal. Chem.* **2018**, *90*, 7086−7093.

(26) Qiu, Z. L.; Shu, J.; Liu, J. F.; Tang, D. P. Dual-channel photoelectrochemical ratiometric aptasensor with up-converting nanocrystals using spatial-resolved technique on homemade 3D printed device. *Anal. Chem.* **2019**, *91*, 1260−1268.

(27) Qiao, L.; Wang, H.; He, J.; Yang, S.; Chen, A. Truncated affinity-improved aptamers for 17β-estradiol determination by AuNPs-based colorimetric aptasensor. *Food Chem.* **2021**, *340*, No. 128181.

(28) Zhou, L.; Ji, F.; Zhang, T.; Wang, F.; Li, Y.; Yu, Z.; Jin, X.; Ruan, B. A fluorescent aptasensor for sensitive detection of tumor marker based on the FRET of a sandwich structured QDs-AFP-AuNPs. *Talanta* **2019**, *197*, 444−450.

(29) Zhang, Y.; Lai, B. S.; Juhas, M. Recent advances in aptamer discovery and applications. *Molecules* **2019**, *24*, 941.

(30) Ma, C. M.; Lin, L. C.; Chuang, K. J.; Hong, G. B. Colorimetric detection of polycyclic aromatic hydrocarbons by using gold nanoparticles. *Spectrochim. Acta, Part A* **2022**, *268*, No. 120701.

(31) Chai, F.; Wang, C. G.; Wang, T. T.; Li, L.; Su, Z. M. Colorimetric detection of Pb^{2+} using glutathione functionalized gold nanoparticles. *ACS. Appl. Mater. Interfaces* **2010**, *2*, 1466−1470.

(32) Chang, C. C.; Chen, C. P.; Wu, T. H.; Yang, C. H.; Lin, C. W.; Chen, C. Y. Gold nanoparticle-based colorimetric strategies for chemical and biological sensing applications. *Nanomaterials* **2019**, *9*, 861.

(33) Aldewachi, H.; Chalati, T.; Woodroofe, M. N.; Bricklebank, N.; Sharrack, B.; Gardiner, P. Gold nanoparticle-based colorimetric biosensors. *Nanoscale* **2018**, *10*, 18−33.

(34) Geleta, G. S. A colorimetric aptasensor based on gold nanoparticles for detection of microbial toxins: an alternative

https://doi.org/10.1021/acsomega.2c08040
ACS Omega 2023, 8, 16000−16008

approach to conventional methods. *Anal. Bioanal. Chem.* **2022**, *414*, 7103−7122.
(35) Ren, R. R.; Cai, G. N.; Yu, Z. Z.; Zeng, Y. Y.; Tang, D. P. Metal-polydopamine framework: an innovative signal-generation tag for colorimetric immunoassay. *Anal. Chem.* **2018**, *90*, 11099−11105.
(36) Gao, Z. Q.; Qiu, Z. L.; Lu, M. H.; Shu, J.; Tang, D. P. Hybridization chain reaction-based colorimetric aptasensor of adenosine 5′-triphosphate on unmodified gold nanoparticles and two label-free hairpin probes. *Biosens. Bioelectron.* **2017**, *89*, 1006−1012.
(37) Zamay, G. S.; Kolovskaya, O. S.; Zamay, T. N.; Glazyrin, Y. E.; Krat, A. V.; Zubkova, O.; Spivak, E.; Wehbe, M.; Gargaun, A.; Muharemagic, D.; Komarova, M.; Grigorieva, V.; Savchenko, A.; Modestov, A. A.; Berezovski, M. V.; Zamay, A. S. Aptamers selected to postoperative lung adenocarcinoma detect circulating tumor cells in human blood. *Mol. Ther.* **2015**, *23*, 1486−1496.
(38) Liu, S.; Xie, T.; Pei, X.; Li, S.; He, Y.; Tong, Y.; Liu, G. CRISPR-Cas12a coupled with universal gold nanoparticle strand-displacement probe for rapid and sensitive visual SARS-CoV-2 detection. *Sens. Actuators, B* **2023**, *377*, No. 133009.
(39) Luan, Y. X.; Chen, J. Y.; Xie, G.; Li, C.; Ping, H.; Ma, Z. H.; Lu, A. X. Visual and microplate detection of aflatoxin B2 based on NaCl-induced aggregation of aptamer-modified gold nanoparticles. *Microchim. Acta* **2015**, *182*, 995−1001.
(40) Jia, J.; Yan, S.; Lai, X.; Xu, Y.; Liu, T.; Xiang, Y. Colorimetric aptasensor for detection of malachite green in fish sample based on RNA and gold nanoparticles. *Food Anal. Methods* **2018**, *11*, 1668−1676.
(41) Liyanage, T.; Lai, M.; Slaughter, G. Label-free tapered optical fiber plasmonic biosensor. *Anal. Chim. Acta* **2021**, *1169*, No. 338629.

https://doi.org/10.1021/acsomega.2c08040
ACS Omega 2023, 8, 16000−16008